

The effect of seawater CO₂ concentration on growth of a natural phytoplankton assemblage in a controlled mesocosm experiment

Ja-Myung Kim and Kitack Lee¹

Pohang University of Science and Technology, School of Environmental Science and Engineering, Pohang, 790-784, Republic of Korea

Kyoungsoon Shin and Jung-Hoon Kang

Korea Ocean Research and Development Institute/South Sea Institute, Jangmok, 656-830, Republic of Korea

Hyun-Woo Lee and Miok Kim

Pohang University of Science and Technology, School of Environmental Science and Engineering, Pohang, 790-784, Republic of Korea

Pung-Guk Jang and Min-Chul Jang

Korea Ocean Research and Development Institute/South Sea Institute, Jangmok, 656-830, Republic of Korea

Abstract

We examine the effects of seawater $p\text{CO}_2$ concentration of 25, 41, and 76 kPa (250, 400, and 750 μatm) on the growth rate of a natural assemblage of mixed phytoplankton obtained from a carefully controlled, 14-d mesocosm experiment. Throughout the experiment period, in all enclosures, two phytoplankton taxa (microflagellates and cryptomonads) and two diatom species (*Skeletonema costatum* and *Nitzschia* spp.) account for approximately 90% of the phytoplankton community. During the nutrient-replete period from day 9 to day 14 populations of *Skeletonema costatum* and *Nitzschia* spp. increased substantially; however, only *Skeletonema costatum* showed an increase in growth rate with increasing seawater $p\text{CO}_2$. Not all diatom species in Korean coastal waters are sensitive to seawater $p\text{CO}_2$ under nutrient-replete conditions.

Since the industrial revolution, human activities have released ever-increasing quantities of CO₂ into the atmosphere. However, only about half of this CO₂ has remained in the atmosphere; the rest has been absorbed into the ocean and land biosphere. The global oceanic sink of fossil-fuel CO₂ has been estimated to be 118 ± 19 petagrams of carbon, accounting for 30% of the total emission during the

period from 1800 to 1994 (Sabine et al. 2004). The fossil-fuel CO₂ absorbed by the ocean is not evenly distributed throughout the depths because it is taken up by the ocean through air–sea gas exchange. The highest concentrations of fossil-fuel CO₂ are found in the upper oceans. Away from the wind-driven upper oceans or deep water formation regions, fossil-fuel CO₂ can only penetrate to deeper depths by slow diffusive processes, and, as a consequence, the concentration of fossil-fuel CO₂ is below the current detection limits in much of the deep ocean (Sabine et al. 2004).

The absorption of fossil-fuel CO₂ has profoundly changed the upper ocean carbonate chemistry (Chung et al. 2004; Feely et al. 2004); for example it has led to an increase in gaseous CO₂ concentration and a decrease in pH and carbonate ion (CO₃²⁻) concentration, which has in turn served to lower the saturation state of seawater with respect to biogenic calcite and aragonite. Over the typical range of surface water pH (7.8–8.2), bicarbonate ions (HCO₃⁻) are a major contributor (~90%) to the total dissolved inorganic carbon concentration ([CO₂] + [HCO₃⁻] + [CO₃²⁻]), followed by CO₃²⁻ (~9%). Less than 1% of the total dissolved inorganic carbon is in the form of gaseous CO₂.

Riebesell et al. (1993) first suggested that some large phytoplankton species may rely on CO₂ diffusion through the cell membrane for growth and, therefore, that the low concentration of CO₂ (5–15 $\mu\text{mol kg}^{-1}$) in the present-day surface ocean would likely hinder phytoplankton growth. When in a low CO₂ environment some phytoplankton

¹ Corresponding author (ktl@postech.ac.kr).

Acknowledgments

We thank two anonymous reviewers and an associate editor, John Raven, for improving the quality of this paper. The success of our mesocosm experiment was attributed to the hard work of the participants over a 2-week period at the South Sea Institute of the Korea Ocean Research and Development Institute in Jangmok, Korea. We thank W.-J. Lee, M.-R. Yun, and other scientific employees of the Korea Ocean Research and Development Institute for helping us set up mesocosms. We also thank M. Chang for his constant encouragement during this experiment. This work was financially supported by the National Research Laboratory (NRL) Program (2005) of the Korea Science and Engineering Foundation and by the Korea Aerospace Research Institute. Partial support for preparation of this manuscript was also provided by the Advanced Environmental Biotechnology Research Center (AEBRC) at Pohang University of Science and Technology (POSTECH), the Brain Korea 21 project, the Korean Science and Engineering Foundation (KOSEF) (R01-2002-000-00549-0, 2004), and the Ministry of education & human resources development (MOEHRD) (KRF-2005-070-C00143).

species can alternatively take up HCO_3^- and convert it to CO_2 in a reaction catalyzed by the enzyme carbonic anhydrase (Kaplan and Reinhold 1999). Therefore, a progressive increase in surface water $p\text{CO}_2$ concentration may lower the metabolic cost for phytoplankton to acquire inorganic carbon, thereby increasing the growth rate of the phytoplankton (Rost et al. 2003; Engel et al. 2005).

The picture of carbon acquisition by phytoplankton outlined above has been challenged in several independent studies, which have suggested that dissolved inorganic carbon is not a limiting factor for marine primary production (e.g., Raven and Johnston 1991; Falkowski 1994). The concentration of gaseous CO_2 ($\sim 10 \mu\text{mol kg}^{-1}$) in seawater equilibrated with the present-day atmospheric $p\text{CO}_2$ is significantly lower than the half-saturation constant of ribulose-1,5-bisphosphate carboxylase/oxygenase (Rubisco, $K_m = 20\text{--}200 \mu\text{mol kg}^{-1}$) (Badger et al. 1998), a key enzyme in carbon fixation. To overcome both the low concentrations of gaseous CO_2 in seawater and the low CO_2 affinity of Rubisco, many marine phytoplankton species increase their intracellular CO_2 concentrations by means of carbon concentrating mechanisms (Raven 1997; Raven and Falkowski 1999; Tortell et al. 2000).

Data on the effect of $p\text{CO}_2$ on phytoplankton growth derived from the numerous laboratory and field experiments that have been performed over the past two decades are difficult to fully reconcile. A carefully controlled mesocosm experiment would potentially be useful for testing the effect of $p\text{CO}_2$ elevation on phytoplankton growth because the mesocosm approach can offer experimental conditions that are as close as possible to the natural environment in terms of fluctuations of light and temperature. Previously, mesocosm experiments have been conducted to investigate the effects of increased $p\text{CO}_2$ on calcification rates of selected marine organisms (Engel et al. 2005), on the elemental composition (C : N : P) of phytoplankton (Burkhardt et al. 1999; Engel et al. 2002), on the accumulation of chromophoric dissolved organic matter (Rochelle-Newall et al. 2004), and on the temporal changes of transparent exopolymer and dissolved organic carbon production (Engel et al. 2004). However, only a few mesocosm-based studies have examined the effects of increasing $p\text{CO}_2$ on the growth rate of a natural phytoplankton assemblage (Engel et al. 2005). The knowledge gained from additional mesocosm-based studies would allow us to predict the response of marine ecosystems to elevated $p\text{CO}_2$ concentrations.

In this paper we present results from a controlled mesocosm experiment that was performed to investigate the growth rate enhancement of a natural assemblage of mixed phytoplankton in response to rising seawater $p\text{CO}_2$, encompassing concentrations ranging from preindustrial levels to those predicted for the year 2100. The response of two diatom species to rising levels of seawater $p\text{CO}_2$ was investigated under the nutrient-replete conditions.

Analytical methods

Mesocosm setup and sampling—The present mesocosm experiment was conducted for 14 d, between 26 November

and 09 December 2004, at the South Sea Institute of the Korea Ocean Research and Development Institute in Jangmok (34.6°N and 128.5°W), located near the southern coast of Korea. Nine impermeable polyethylene enclosures (0.53 m in diameter and 0.8 m in height) were moored to a polyethylene float. Prior to filling the enclosures, about 2,000 liters of seawater was pumped from a depth of 1 m adjacent to the floating frame, passed through a filter with a pore size of 60 μm in order to remove most zooplankton and higher trophics, and then stored in a 2,500-liter sample container. To minimize possible differences in cell concentration between the nine enclosures in the initial phase, all enclosures were simultaneously filled from the 2,500-liter sample container, with each enclosure receiving ~ 150 liters of the filtered seawater. The mesocosm system and ancillary components are not shown here because they are similar to those used by Engel et al. (2005), with the exception that our enclosures were considerably smaller than theirs ($\sim 11,000$ liters).

After filling the enclosures with filtered seawater, the seawater $p\text{CO}_2$ levels in the enclosures were manipulated to achieve three levels, with each $p\text{CO}_2$ level being replicated in three enclosures. The three target $p\text{CO}_2$ values of 25, 41, and 76 kPa (250, 400, and 750 μatm) were chosen to simulate the preindustrial, present-day, and predicted year 2100 atmospheres, respectively. The $p\text{CO}_2$ value of 76 kPa for the year 2100 atmospheric CO_2 concentration was chosen on the basis of model projections under the “business-as-usual” scenario (Houghton et al. 2001). Within a day, the target seawater $p\text{CO}_2$ levels were achieved by bubbling either nitrogen (99.999%), ambient air, or air containing 3% CO_2 through the seawater via 0.5-mm porous tubes (~ 2 m in perimeter and ~ 1 cm in diameter). Once the target seawater $p\text{CO}_2$ concentrations were achieved, the atmospheric $p\text{CO}_2$ levels in the mesocosms were manipulated to achieve the target values by continuously releasing into the mesocosm atmosphere air with the appropriate $p\text{CO}_2$ value (25, 41, or 76 kPa). The enclosures were not completely sealed on their tops, thereby avoiding overpressure within the enclosures during the CO_2 -containing air release process.

Because the process of measuring seawater $p\text{CO}_2$ using an infrared/equilibrating-based $p\text{CO}_2$ measurement system has the unwanted effect of removing phytoplankton cells from the enclosures, we used uncalibrated pH as a surrogate for $p\text{CO}_2$ in the seawater samples within the enclosures. Hence, in the 14-d experiment period, uncalibrated pH in seawaters within the enclosures was continuously measured using pH electrodes that provide millivolt (mV) signals proportional to pH. The pH sensors then internally converted the measured millivolts to pH values using a theoretical slope of -59.16 mV per unit pH change and a signal of 0 mV at $\text{pH} = 7.0$ for all electrodes. The resulting seawater pH values in the enclosures were then converted to the corresponding $p\text{CO}_2$ levels using pH– $p\text{CO}_2$ relationships derived from uncalibrated pH values measured on seawater samples with known $p\text{CO}_2$ values (Fig. 1). The pH– $p\text{CO}_2$ relationships derived for the nine pH electrodes differed slightly because each pH electrode has a unique Nernstian slope, and therefore

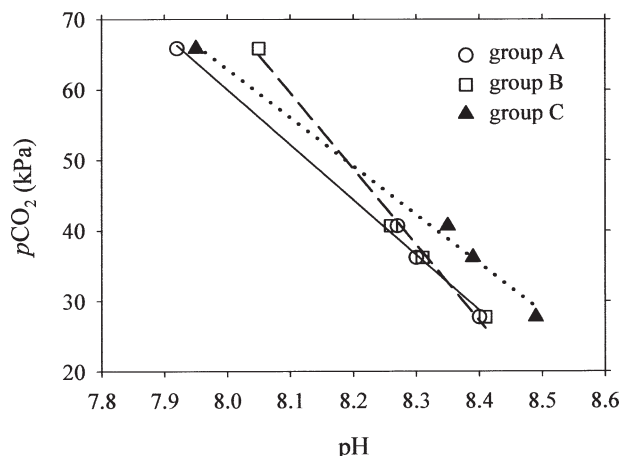


Fig. 1. pH– $p\text{CO}_2$ relationships derived from pH and $p\text{CO}_2$ measurements conducted on the same seawater samples with varying $p\text{CO}_2$ values covering 26 to 68 kPa. These empirical pH– $p\text{CO}_2$ relationships were used to convert measured seawater pH values to $p\text{CO}_2$. Each group consisted of three enclosures; the enclosures in each group were treated with the same $p\text{CO}_2$ concentration (25, 41, or 76 kPa). Shown are three representative pH– $p\text{CO}_2$ relationships derived for one enclosure from each group.

a unique trend with changing $p\text{CO}_2$. We only directly measured the seawater $p\text{CO}_2$ in the enclosures using the infrared/equilibrators-based $p\text{CO}_2$ system immediately after the final sampling on day 14. The directly measured $p\text{CO}_2$ values were consistent with those obtained using the pH measurements and pH– $p\text{CO}_2$ relationships. The infrared/equilibrators-based $p\text{CO}_2$ system used in the present study is similar to one developed by Wanninkhof and Thoning (1993). This system measures CO₂ concentration using a Li-Cor (model 820) infrared analyzer in air that reached equilibrium with the seawater sample within the equilibrator.

During the prebloom period (days 1–8), the N concentration in all enclosures was lower than $0.2 \mu\text{mol kg}^{-1}$, whereas the P and Si concentration remained ~ 0.2 and $\sim 10 \mu\text{mol kg}^{-1}$, respectively. To initiate the development of a bloom in the final phase of the experiment (days 9–14), the same amount of a NaNO₃–Na₂HPO₄ mixture was added to each enclosure on day 8, yielding concentrations of $\sim 23 \mu\text{mol kg}^{-1}$ nitrate (N) and $\sim 0.9 \mu\text{mol kg}^{-1}$ phosphate (P). Subsequent to the nutrient addition, the concentrations of N, P, and Si decreased sharply during the remaining period. All enclosures were sampled daily at $\sim 15:00$ h from ~ 1 m depth for 14 d, starting the day (day 1) before the seawater $p\text{CO}_2$ in all enclosures reached the target values on day 2.

The bay in which the enclosures were located is surrounded by several islands, which suppressed wind-driven turbulence within the bay. Therefore, the seawater within each enclosure was not vigorously mixed to ensure homogeneity of the phytoplankton population. To minimize the possibility of sampling bias due to inhomogeneous distribution of phytoplankton within the enclosure being sampled, the seawater in each enclosure was mechanically mixed before sampling.

Measured parameters—A total of 2 liters of seawater was taken from each enclosure for measurements of biological parameters. An aliquot (~ 500 mL) of the seawater sample was preserved with Lugol's iodine solution and analyzed immediately after the mesocosm experiment using a light microscope equipped with a Sedgwick Rafter counting chamber. Using this apparatus, we identified the dominant phytoplankton groups and determined their concentrations as well as the cell concentrations of other phytoplankton species. The phytoplankton identification and cell counting procedure was repeated three times for each sample. For each species, the mean cell concentration obtained by averaging the three separate cell counts was used to calculate the net growth rate of that species. The average uncertainty in cell counting was less than 10% of the total population of each species. The mean growth rate (μ) for each phytoplankton taxa or species during the study period was calculated from regressions of plots of the natural logarithm of the daily cell count against time, and the uncertainties in the values obtained were taken as the standard errors of the regression coefficients. Samples for nutrient analysis (NH₄⁺, NO₃[−], NO₂[−], HPO₄^{2−}, and Si(OH)₄) were collected by filtration through a Whatman GF/F filter of pore size $0.7 \mu\text{m}$ and were analyzed using a flow injection analyzer (Quickchem 8000) (Parsons et al. 1984).

For particulate organic carbon (POC) and nitrogen (PON) collections and analysis, suspended particles were collected on glass fiber filters with a nominal pore size of $0.7 \mu\text{m}$ (Karl et al. 1991; UNESCO 1994). Duplicate samples were taken for the POC and PON determinations. After filtration, the wet filters were dislodged from the filter holders with a pair of stainless steel tweezers and placed into a shallow cavity in a clean Plexiglas transport box. The transport box containing the wet filters was then dried at $\sim 50^\circ\text{C}$ for 2 d. Immediately prior to analysis, using a clean pair of tweezers, the dried filters were folded in Sn foil and palletized. A CHN elemental analyzer (ThermoFinnigan, EA1112) was used to determine the amounts of POC and PON on the dried filters. The technical details of the CHN analyzer are given elsewhere (Sharp 1974).

For dissolved organic carbon (DOC) analysis, each seawater sample was filtered through a precombusted GF/F $0.7\text{-}\mu\text{m}$ filter and 20 mL of the filtered sample was collected in a precombusted 30-mL glass vial (Corning 430052). After collection, the filtered seawater sample was immediately acidified with $\sim 10\%$ H₃PO₄ solution and purged with ultrapure O₂ gas for ~ 10 min to remove dissolved inorganic carbon (DIC). One hundred microliters of the DIC-free subsample was then injected into the combustion tube of a Shimadzu TOC-V_{CPH} total organic carbon analyzer for the oxidation of DOC to CO₂, which was facilitated by a platinum catalyst at 650°C . The liberated CO₂ was subsequently measured using an infrared detector. On each day measurements were performed, a three-point calibration curve was constructed using potassium phthalate standards freshly prepared in Milli-Q water. These standards covered a DOC concentration range of 0 to $830 \mu\text{mol kg}^{-1}$ and were run once per

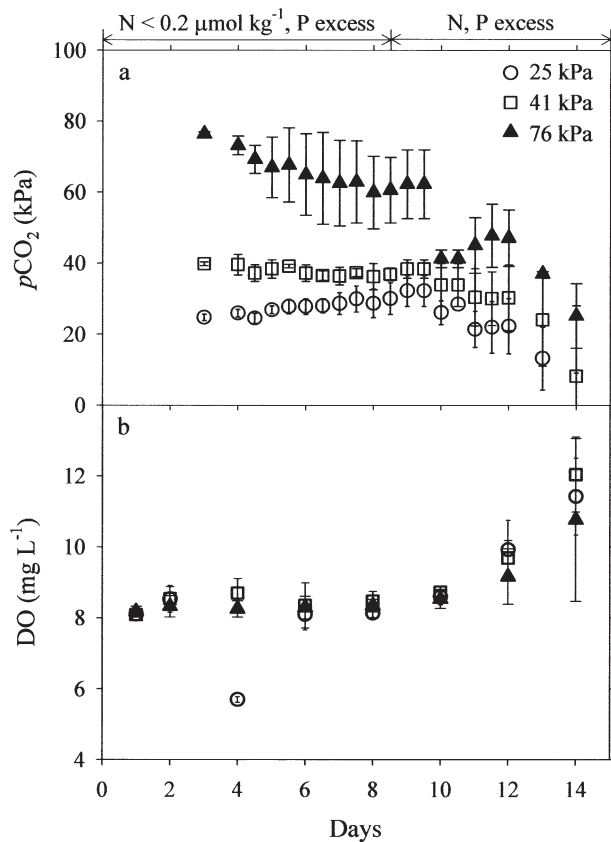


Fig. 2. Seawater (a) $p\text{CO}_2$ (kPa) and (b) dissolved O_2 (DO) (mg L^{-1}) values in the enclosures over the 14-d experiment period. Circles and squares represent the preindustrial (~ 25 kPa) and present (~ 41 kPa) atmospheres, respectively. Filled triangles represent the year 2100 atmosphere (~ 76 kPa). Error bars represent the standard deviation of the mean results of the replicate enclosures.

day. All DOC measurements reported here represent the mean of three injections from each sample.

Throughout the mesocosm experiment, the temperature and salinity in the enclosures were measured daily using a SeaBird 19 conductivity–temperature–density profiler. In particular, the salinity measurements were used to check for changes in salinity indicative of sample contamination from sources such as inadvertent introduction of adjacent bay waters. One of the enclosures treated with 76-kPa $p\text{CO}_2$ was found to have been contaminated with bay water through holes in the enclosure. Therefore, data collected from this defective enclosure were not used in the present study.

Statistical treatment of results—Data obtained from the mesocosm experiments were treated with analysis of variance (ANOVA). To determine whether changes in the growth rate of phytoplankton in response to changes in seawater $p\text{CO}_2$ were statistically significant, the ANOVA compared the differences among the growth rates within enclosures treated with the same $p\text{CO}_2$ with those among the three different $p\text{CO}_2$ treatments by calculating the F value (Keller and Warrack 1999). If the p value is smaller

than 0.05, the ANOVA test suggests that the growth rate of the phytoplankton tested in our experiment is sensitive to the seawater $p\text{CO}_2$ concentration.

Results and discussion

Atmospheric and seawater $p\text{CO}_2$ within the enclosures—The atmospheric and seawater $p\text{CO}_2$ levels in the mesocosms reached their target values by day 3 of the 14-d experiment. After this initial adjustment period, the atmospheric $p\text{CO}_2$ levels in the mesocosms were maintained close to the target values by continuously releasing air with the appropriate $p\text{CO}_2$ value of 25, 41, or 76 kPa (250, 400, or 750 μatm) into the atmosphere of each mesocosm. By contrast, the seawater $p\text{CO}_2$ levels in the mesocosms decreased with time (Fig. 2a), largely because of photosynthetic use of carbon, as shown in the next section.

The seawater $p\text{CO}_2$ values in the enclosures treated initially with 25- and 41-kPa $p\text{CO}_2$ remained close to target values from days 3 to 8 (Fig. 2a). By contrast, the seawater $p\text{CO}_2$ in the 76-kPa-treated enclosures decreased significantly from ~ 76 kPa on day 3 to ~ 66.9 kPa on day 5 and remained approximately constant thereafter (days 5–8) (Fig. 2a). Over the initial 8 d, the seawater temperature in all enclosures decreased by $\sim 1^\circ\text{C}$ from 15°C on day 1 to 14°C on day 8. This temperature decrease that occurred in all enclosures during this period would be expected to lower the seawater $p\text{CO}_2$ to the observed level. The temperature-induced change in seawater $p\text{CO}_2$ can be approximated as a $\sim 4.2\%$ decrease in seawater $p\text{CO}_2$ per $^\circ\text{C}$ temperature decrease (Takahashi et al. 1993; Lee and Millero 1995; Lee et al. 1996). Our observation of a negligible change in seawater $p\text{CO}_2$ in the enclosures treated with 25- and 41-kPa $p\text{CO}_2$ suggests that the flux of CO_2 from the mesocosm atmosphere approximately compensated for the $p\text{CO}_2$ reduction due to the temperature decrease. The more complicated trend we observed in the seawater $p\text{CO}_2$ in the 76-kPa-treated enclosures—a decrease from ~ 76 kPa on day 3 to ~ 66.9 kPa on day 5 followed by approximately constant $p\text{CO}_2$ from days 5 to 8 (Fig. 2a)—can be accounted for as follows. The approximately 9 kPa decrease in seawater $p\text{CO}_2$ from days 3 to 5 was probably due to efflux of CO_2 from the 76-kPa-treated enclosures caused by occasional failures in the system controlling the mesocosm atmospheric $p\text{CO}_2$ values. The nearly constant seawater $p\text{CO}_2$ in the 76-kPa-treated enclosures from days 5 to 8 suggests that, during this period, the flux of CO_2 from the mesocosm atmosphere approximately compensated for the $p\text{CO}_2$ reduction due to a decrease in temperature.

Following the addition of N and P to the mesocosms on day 8, a significant reduction in seawater $p\text{CO}_2$ occurred in all enclosures that continued until the end of the experiment. During this period, the seawater $p\text{CO}_2$ in the enclosures decreased substantially, by ~ 15 kPa for the 25-kPa-treated enclosures, ~ 25 kPa for the 41-kPa-treated enclosures, and ~ 23 kPa for the 76-kPa-treated enclosures. The decrease in seawater temperature over this time period was too small (less than 0.5°C) to account for the observed decrease in seawater $p\text{CO}_2$. Therefore, the large decreases in

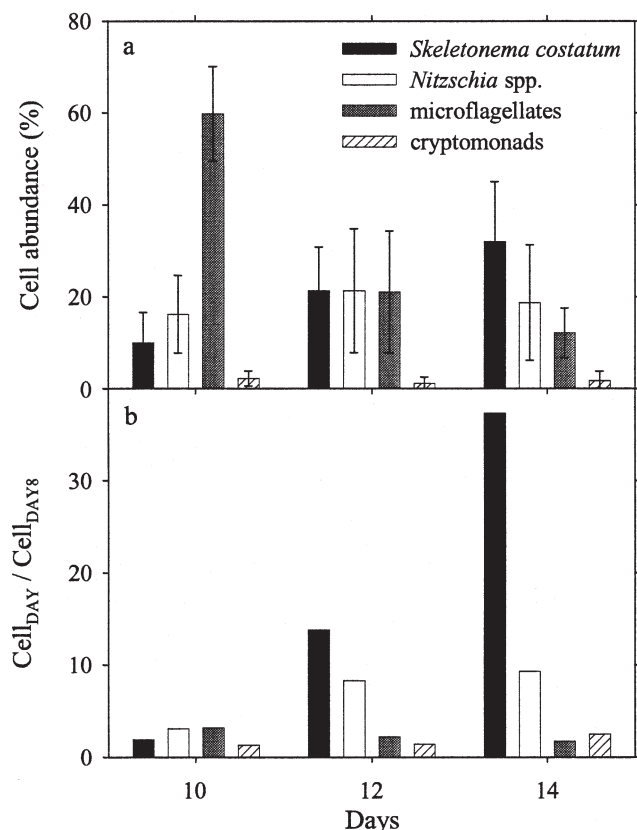


Fig. 3. (a) Relative cell contributions (%) of the four major phytoplankton populations to the total phytoplankton during the bloom period (days 9–14) and (b) their cell concentration changes relative to their mean cell concentrations on day 8 (Cell_{DAY8}) (i.e., prior to nutrient addition). Error bars for the relative cell abundance data in (a) are standard deviations from the mean cell populations for eight enclosures (two sets of triplicates, 25- and 41-kPa $p\text{CO}_2$ treatments; and one set of duplicates, 76-kPa $p\text{CO}_2$ treatment). The experiment period was split into the prebloom phase (days 1–8) and the bloom phase (days 9–14).

seawater $p\text{CO}_2$ in the enclosures can be attributed to photosynthetic use of CO₂.

During the N₂ bubbling process over a day (day 3), the seawater O₂ concentrations in the 25-kPa-treated enclosures decreased by ~18%, compared with those in the 41-kPa- and 76-kPa-treated enclosures (Fig. 2b). This decrease in O₂ concentrations occurred only in the 25-kPa-treated enclosures because the other sets of enclosures were treated with air containing O₂ and target concentrations of CO₂ (41 and 76 kPa). However, within 2 d after the cessation of N₂ bubbling through the seawater samples, the seawater O₂ concentrations in the 25-kPa-treated enclosures rapidly reached the levels achieved by the other two treatments (Fig. 2b). Such rapid recovery in O₂ concentrations in the 25-kPa-treated enclosures is primarily due to the rapid flux of O₂ from the atmosphere. Since our interpretation focuses on results collected during the exponential growth period (days 9–14), the decrease in O₂ concentrations in the 25-kPa-treated enclosures in the earlier phase of the experiment probably does not affect our interpretation.

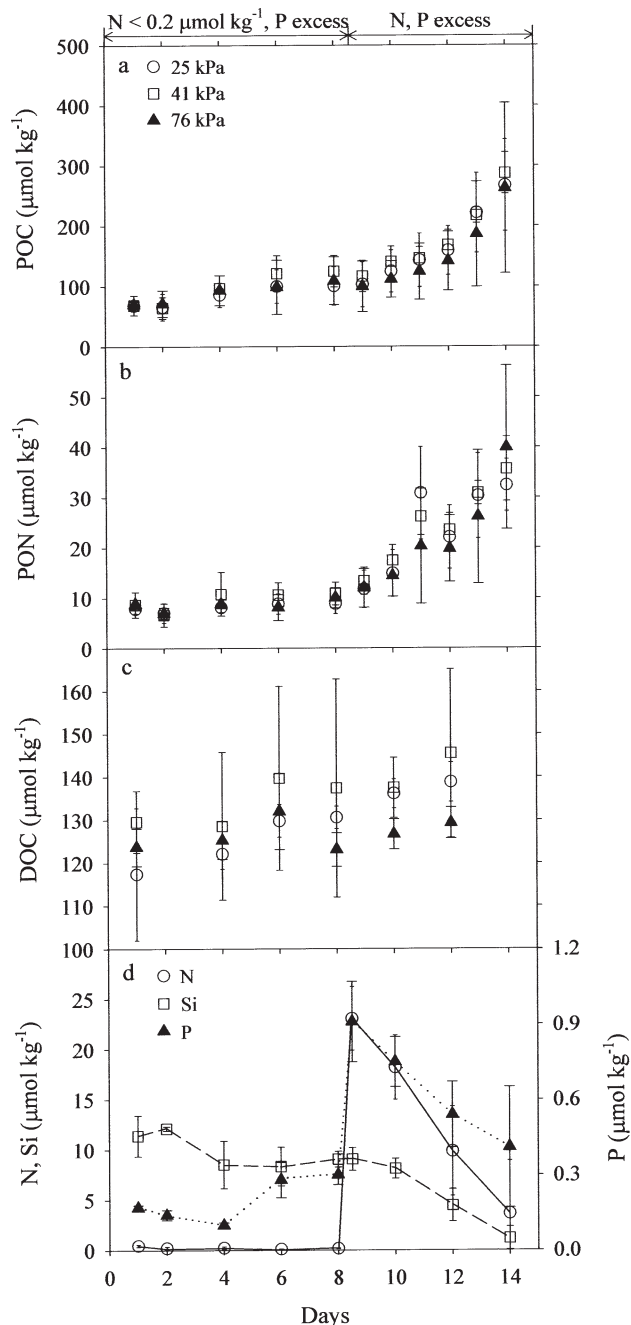


Fig. 4. Changes in (a) particulate organic carbon (POC), (b) particulate organic nitrogen (PON), (c) dissolved organic carbon (DOC), and (d) nitrate (N), silicate (Si), and phosphate (P) concentrations during the study period. The experiment period was split into the prebloom phase (days 1–8) and the bloom phase (days 9–14). Error bars represent the standard deviations of the mean results of the replicate enclosures.

Population dynamics of phytoplankton—In all enclosures during the prebloom period (days 1–8), two phytoplankton taxa (microflagellates and cryptomonads) and two diatom species (*Skeletonema costatum* and *Nitzschia* spp.) accounted for approximately 90% of the phytoplankton community (Fig. 3a). Microflagellates were by far the largest contributor, accounting for more than 50% of the

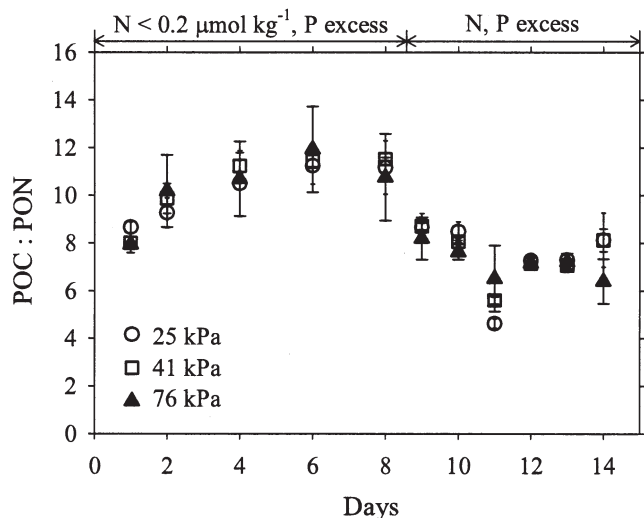


Fig. 5. The elemental molar ratios of POC : PON as a function of time during the study period, which was split into the prebloom phase (days 1–8) and the bloom phase (days 9–14). Error bars represent the standard deviations of the mean results of the replicate enclosures.

total phytoplankton community, followed by *S. costatum*, *Nitzschia* spp., and cryptomonads. The N concentration remained lower than $0.2 \mu\text{mol kg}^{-1}$ in all enclosures, which was the primary factor limiting phytoplankton growth during this period. After the addition of N and P on day 8, all mesocosms contained excess amounts of N and P throughout the remainder of the experiment (days 9–14) (Fig. 4d). The Si concentration remained approximately $10 \mu\text{mol kg}^{-1}$ during the prebloom period and subsequently decreased to less than $2 \mu\text{mol kg}^{-1}$ during the exponential growth period. Under this nutrient-replete condition, both *S. costatum* and *Nitzschia* spp. showed significant increases in relative cell abundance and cell density in all enclosures (Fig. 3). By contrast, the relative abundances and cell concentrations of microflagellates, which were the dominant phytoplankton taxa during the prebloom period, decreased substantially between day 8 and day 14 in all enclosures (Fig. 3).

Although the seawater was filtered when the enclosures were filled on the first day of the experiment, some dinoflagellates were missed by the filtration process. Under the optimum nutrient conditions, these remaining dinoflagellates could potentially cause a decrease in the cell concentrations of microflagellates and cryptomonads. The presence of dinoflagellates was confirmed by the observation of five such organisms, *Akashiwo sanguinea*, *Prorocentrum triestinum*, *Protoperidinium bipes*, *Pleurobema pyriforme*, and *Scrippsiella trochoidea*, in all enclosures throughout the experiment period. These dinoflagellates are known as mixotrophic (Jeong and Latz 1994; Jacobson and Anderson 1996; Stoecker et al. 1997). Although we did not attempt to quantify the dinoflagellate-induced grazing pressure on microflagellates, the presence of these dinoflagellates in all enclosures during the nutrient-replete period may explain, at least in part, the decrease in microflagellate cell concentrations during this period. By

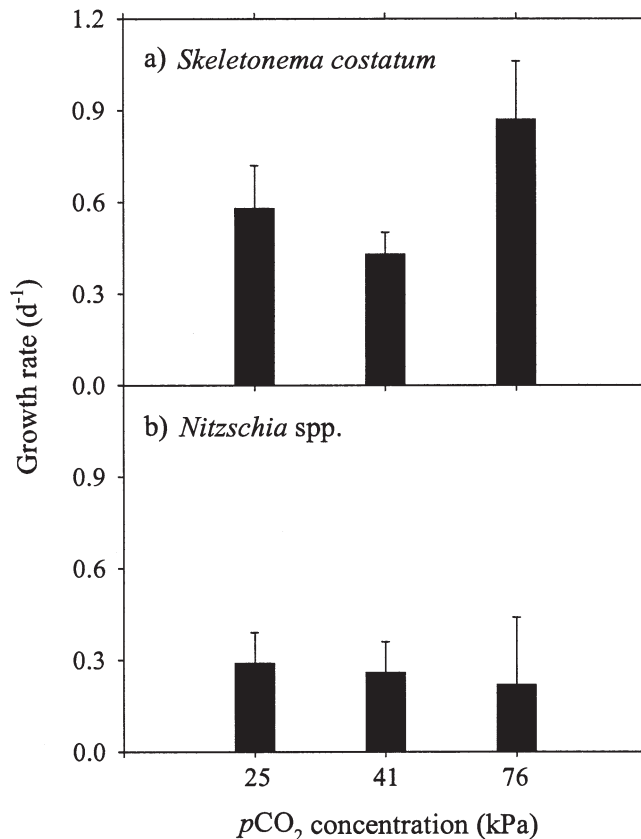


Fig. 6. The effects of varying $p\text{CO}_2$ concentrations on the mean growth rates of (a) *S. costatum*, and (b) *Nitzschia* spp. during the bloom period. Error bars represent the standard deviations from the mean growth rates of the replicate enclosures. The growth rate for each enclosure was estimated using linear regression analysis of natural log transformed cell populations measured during the exponential growth period (days 9–14).

contrast, no herbivorous copepods that would graze on *S. costatum* and *Nitzschia* spp. were found in any of the enclosures, indicating that they were removed by the filtration process.

Production of POC, PON, and DOC—During the prebloom period, only a slight increase in the net growth of the phytoplankton population was observed in all enclosures, as reflected in the POC and PON concentrations (Fig. 4a,b). Following the injection of N and P into all enclosures on day 8, the phytoplankton population increased exponentially and, as a result, the POC concentration increased substantially from a prebloom value of ~ 110 to $\sim 270 \mu\text{mol kg}^{-1}$ at the height of the bloom (Fig. 4a). Parallel to this, the PON concentrations in the enclosures also increased sharply from a prebloom value of ~ 16 to $\sim 35 \mu\text{mol kg}^{-1}$ at the height of the bloom (Fig. 4b). The variability of POC and PON productions among the enclosures was small during the N-depleted period and then increased as the bloom progressed. During the later stage of the exponential growth phase (days 11–14), the increase in POC production was stoichiometrically related to the increase in PON production, causing the molar

Table 1. Effects of pCO₂ manipulation on the growth rates of *Skeletonema costatum* and *Nitzschia* spp. found in Korean coastal waters.

Phytoplankton population	pCO ₂	Growth rate (d ⁻¹) ± SE*		
		25 kPa (250 μatm)	41 kPa (400 μatm)	76 kPa (750 μatm)
<i>Skeletonema costatum</i>	A	0.61 ± 0.20*	0.48 ± 0.00	0.73 ± 0.13
	B	0.43 ± 0.15	0.36 ± 0.12	1.00 ± 0.23
	C	0.69 ± 0.14	0.46 ± 0.10	
	mean	0.58 ± 0.16†	0.43 ± 0.07	0.87 ± 0.18
<i>Nitzschia</i> spp.	A	0.23 ± 0.04*	0.15 ± 0.08	0.38 ± 0.18
	B	0.23 ± 0.20	0.33 ± 0.16	0.07 ± 0.16
	C	0.40 ± 0.08	0.31 ± 0.12	
	mean	0.29 ± 0.11†	0.26 ± 0.12	0.22 ± 0.17

* Standard error = (the sum of squared deviations/(n - 2))^{1/2}.

† Means of standard errors.

POC : PON ratio to remain constant (~7) (Redfield et al. 1963) (Fig. 5).

Although the majority of photosynthetic production goes into the growth of phytoplankton, a fraction can leak out or be excreted as DOC (Carlson 2002). During the prebloom period, the concentration of DOC was ~129 ± 13 μmol kg⁻¹ in all enclosures, and this concentration increased by only ~5 μmol kg⁻¹ in all enclosures during the exponential growth phase (days 9–14) (Fig. 4c). One can also construct the carbon mass balance during the exponential growth phase. The biological drawdown in dissolved inorganic carbon concentration (ΔC_{T-BIO}) within each enclosure equates to the combined production of particulate (ΔPOC) and dissolved (ΔDOC) organic carbon:

$$\Delta C_{T-BIO} = \Delta POC + \Delta DOC \quad (1)$$

where ΔC_{T-BIO} is calculated from the reduction in N concentration using the mean measured POC : PON ratio of 7.5. The N-based estimates of ΔC_{T-BIO} for all enclosures are in reasonable agreement with the combined production of POC and DOC within 24% of the total production. The net production of DOC accounts for ~2% of the total POC production during the exponential growth period.

The effect of CO₂ on the phytoplankton growth rate—Our results suggest that there were no clear differences in POC accumulation across the pCO₂ treatments (Fig. 4a), nor were there differences in DOC accumulation (Fig. 4c). A possible explanation for this apparent lack of a CO₂ effect is that because changes in the POC and DOC pools represent changes in the entire phytoplankton community, they do not properly reflect a species-specific response to pCO₂ elevation.

To evaluate the response of each phytoplankton species to the pCO₂ manipulation, we examined the net growth rate of each phytoplankton species calculated from daily phytoplankton cell counts during the nutrient-replete period (days 9–14). Microzooplankton grazing on microflagellates and cryptomonads likely affected the cell concentrations of these organisms and, as a result, the present experiment was not adequate to test whether they show growth rate enhancement in response to increases in pCO₂. Only the populations of two diatoms—*S. costatum*

and *Nitzschia* spp.—increased substantially in response to the addition of N and P on day 8.

During the exponential growth period, a mean growth rate of *S. costatum* was 0.58 ± 0.14 d⁻¹ in the 25-kPa pCO₂ treatment, 0.43 ± 0.07 d⁻¹ in the 41-kPa pCO₂ treatment, and 0.87 ± 0.19 d⁻¹ in the 76-kPa pCO₂ treatment (Fig. 6a; Table 1). The difference in growth rate between 25- and 41-kPa pCO₂ treatments was not statistically significant (ANOVA, *p* = 0.098); however, the growth rates under the 25- and 41-kPa pCO₂ treatment conditions did differ significantly from that of the 76-kPa pCO₂ treatment (ANOVA, *p* = 0.038), indicating that *S. costatum* showed a response to the pCO₂ treatment. The pCO₂-induced growth enhancement was calculated by dividing the average of the mean growth rates obtained for the 25- and 41-kPa pCO₂ treatments by the mean rate obtained for the 76-kPa pCO₂ treatment ($[(\bar{\mu}_{25} + \bar{\mu}_{41})/2 - \bar{\mu}_{76}]/\bar{\mu}_{76} \times 100$). In this calculation, we assumed that the mean growth rates obtained from both the 25- and 41-kPa pCO₂ treatments can be combined because the measured seawater pCO₂ values for the enclosures treated with 25- and 41-kPa pCO₂ differed on average by less than 6 kPa. By contrast, the measured seawater pCO₂ values for the 76-kPa pCO₂ treatments were on average 20 kPa higher than those for the 41-kPa treatments. The results of this calculation indicate that the mean growth rate of *S. costatum* increased by ~40% (±25%) in response to a rise in pCO₂ levels, with other factors remaining constant. A similar growth rate enhancement under high pCO₂ conditions was observed in previous laboratory culture studies on the same species (Burkhardt and Riebesell 1997; Burkhardt et al. 1999).

By contrast, *Nitzschia* spp. exhibited an approximately constant growth rate of 0.25 ± 0.02 d⁻¹ across all of the pCO₂ treatments (Fig. 6b; Table 1). The lack of significant differences in growth rate of *Nitzschia* spp. among the three treatments (ANOVA, *p* = 0.871) indicates that the growth rate of this organism is insensitive to the seawater pCO₂ level. The different responses of *S. costatum* and *Nitzschia* spp. to seawater pCO₂ manipulation suggest that future increases in pCO₂ in the surface ocean could potentially change the structure of the diatom population.

In the present mesocosm experiment, we examined the effect of varying $p\text{CO}_2$ levels on the net growth of a natural phytoplankton assemblage over a long period (14 d). The addition of N and P into all mesocosms on day 8 created an artificial bloom during the final phase of the experiment (days 9–14). Our results suggest that two diatom species in the phytoplankton assemblage responded differently when exposed to varying $p\text{CO}_2$ levels, with only *S. costatum* showing an enhanced growth rate in response to $p\text{CO}_2$ elevation.

References

- BADGER, M. R., T. J. ANDREWS, S. M. WHITNEY, M. LUDWIG, D. C. YELLOWLEES, W. LEGGAT, AND G. D. PRICE. 1998. The diversity and coevolution of Rubisco, plastids, pyrenoids, and chloroplast-based CO_2 -concentrating mechanisms in algae. *Can. J. Bot.* **76**: 1052–1071.
- BURKHARDT, S., AND U. RIEBESELL. 1997. CO_2 availability affects elemental composition (C:N:P) of the marine diatom *Skeletonema costatum*. *Mar. Ecol. Prog. Ser.* **155**: 67–76.
- , ———, AND I. ZONDERVAN. 1999. Effects of growth rate, CO_2 concentration, and cell size on the stable carbon isotope fractionation in marine phytoplankton. *Geochim. Cosmochim. Acta* **63**: 3729–3741.
- CARLSON, C. A. 2002. Production and removal processes, p. 91–139. *In* D. A. Hansell and C. A. Carlson [eds.], *Biogeochemistry of marine dissolved organic matter*. Academic.
- CHUNG, S.-N., AND OTHERS. 2004. Postindustrial enhancement of aragonite undersaturation in the upper tropical and subtropical Atlantic Ocean: The role of fossil fuel CO_2 . *Limnol. Oceanogr.* **49**: 315–321.
- ENGEL, A., B. DELILLE, S. JACQUET, U. RIEBESELL, E. ROCHELLE-NEWALL, A. TERBRÜGGEN, AND I. ZONDERVAN. 2004. Transparent exopolymer particles and dissolved organic carbon production by *Emiliania huxleyi* exposed to different CO_2 concentrations: A mesocosm experiment. *Aquat. Microb. Ecol.* **34**: 93–104.
- , S. GOLDTHWAIT, U. PASSOW, AND A. ALLDREDGE. 2002. Temporal decoupling of carbon and nitrogen dynamics in a mesocosm diatom bloom. *Limnol. Oceanogr.* **47**: 753–761.
- , AND OTHERS. 2005. Testing the direct effect of CO_2 concentration on a bloom of the coccolithophorid *Emiliania huxleyi* in mesocosm experiments. *Limnol. Oceanogr.* **50**: 493–507.
- FALKOWSKI, P. G. 1994. The role of phytoplankton photosynthesis in global biogeochemical cycles. *Photosynth. Res.* **39**: 235–258.
- FEELY, R. A., C. L. SABINE, K. LEE, W. BERELSON, J. KLEYPAS, V. J. FABRY, AND F. J. MILLERO. 2004. Impact of anthropogenic CO_2 on the CaCO_3 system in the oceans. *Science* **305**: 362–366.
- HOUGHTON, J. T., Y. DING, D. J. GRIGGS, M. NOGUER, P. J. VAN DER LINDEN, AND D. XIAOSU. 2001. *Climate change 2001: The scientific basis*. Cambridge Univ. Press.
- JACOBSON, D. M., AND D. M. ANDERSON. 1996. Widespread phagocytosis on ciliates and other protists by marine mixotrophic and heterotrophic thecate dinoflagellates. *J. Phycol.* **32**: 279–285.
- JEONG, H. J., AND M. I. LATZ. 1994. Growth and grazing rates of the heterotrophic dinoflagellates *Protoperdinium* spp. on red tide dinoflagellates. *Mar. Ecol. Prog. Ser.* **106**: 173–185.
- KAPLAN, A., AND L. REINHOLD. 1999. CO_2 concentrating mechanisms in photosynthetic microorganisms. *Annu. Rev. Plant Physiol. Plant Mol. Biol.* **50**: 539–570.
- KARL, D. M., B. D. TILBROOK, AND G. TIEN. 1991. Seasonal coupling of organic matter production and particle flux in the western Bransfield Strait, Antarctica. *Deep-Sea Res.* **38**: 1097–1126.
- KELLER, G., AND B. WARRACK. 1999. *Statistics for management and economics*. Duxbury.
- LEE, K., AND F. J. MILLERO. 1995. Thermodynamic studies of the carbonate system in seawater. *Deep-Sea Res.* **42**: 2035–2061.
- , ———, AND D. M. CAMPBELL. 1996. The reliability of the thermodynamic constants for the dissociation of carbonic acid in seawater. *Mar. Chem.* **55**: 233–245.
- PARSONS, T. R., Y. MAITA, AND C. M. LALLI. 1984. *A manual of chemical and biological methods for seawater analysis*. Pergamon.
- RAVEN, J. A. 1997. Inorganic carbon acquisition by marine autotrophs. *Adv. Bot. Res.* **27**: 85–209.
- , AND P. G. FALKOWSKI. 1999. Oceanic sinks for atmospheric CO_2 . *Plant. Cell Environ.* **22**: 741–755.
- , AND A. M. JOHNSTON. 1991. Mechanisms of inorganic carbon acquisition in marine phytoplankton and their implications for the use of other resources. *Limnol. Oceanogr.* **36**: 1701–1714.
- REDFIELD, A. C., B. H. KETCHUM, AND F. A. RICHARDS. 1963. The influence of organisms on the composition of seawater, p. 26–77. *In* M. N. Hill [ed.], *The sea: Ideas and observations on progress in the study of the seas*. Wiley-Interscience.
- RIEBESELL, U., D. A. WOLF-GLADROW, AND V. SMETACEK. 1993. Carbon dioxide limitation of marine phytoplankton growth rates. *Nature* **361**: 249–251.
- ROCHELLE-NEWALL, E., AND OTHERS. 2004. Chromophoric dissolved organic matter in experimental mesocosms maintained under different $p\text{CO}_2$ levels. *Mar. Ecol. Prog. Ser.* **272**: 25–31.
- ROST, B., U. RIEBESELL, S. BURKHARDT, AND D. SÜLTEMAYER. 2003. Carbon acquisition of bloom-forming marine phytoplankton. *Limnol. Oceanogr.* **48**: 55–67.
- SABINE, C. L., AND OTHERS. 2004. The oceanic sink for anthropogenic CO_2 . *Science* **305**: 367–371.
- SHARP, J. H. 1974. Improved analysis for “particulate” organic carbon and nitrogen from seawater. *Limnol. Oceanogr.* **19**: 984–989.
- STOECKER, D. K., A. LI, D. W. COATS, D. E. GUSTAFSON, AND M. K. NANNEN. 1997. Mixotrophy in the dinoflagellate *Protoperdinium minimum*. *Mar. Ecol. Prog. Ser.* **152**: 1–12.
- TAKAHASHI, T., J. OLAFSSON, J. G. GODDARD, D. W. CHIPMAN, AND S. C. SUTHERLAND. 1993. Seasonal variation of CO_2 and nutrients in the high-latitude surface oceans: A comparative study. *Glob. Biogeochem. Cycles* **7**: 843–878.
- TORTELL, P. D., G. H. RAU, AND F. M. M. MOREL. 2000. Inorganic carbon acquisition in coastal Pacific phytoplankton communities. *Limnol. Oceanogr.* **45**: 1485–1500.
- UNESCO. 1994. *Protocols for the Joint Global Ocean Flux Study (JGOFS) core measurement*. United Nations Educational, Scientific, and Cultural Organization.
- WANNINKHOF, R., AND K. THONING. 1993. Measurement of fugacity of CO_2 in surface water using continuous and discrete methods. *Mar. Chem.* **44**: 189–204.

Received: 7 November 2005
Accepted: 20 January 2006
Amended: 22 February 2006